American Journal of Applied Sciences 5 (5): 454-460, 2008
ISSN 1546-9239

Creep-Fatigue Crack Growth Interaction in Nickel Base Supper Alloy

F.Djavanroodi
Department of Mechanical Engineering, Iran University of Science and Technology, Tehran, Iran

Abstract: Most engineering components which operate at elevated temperatures are subjected to non-steady loading during service. This paper describes the current fracture mechanics concepts that are employed to predict cracking of Nickel base supper alloy materials at high temperatures under low and high frequency cyclic loading. A model for predicting creep crack growth in terms of C* and the creep uniaxial ductility is presented at low frequency and at high frequency power law relation is used to predict the crack growth rate. When dealing with creep/fatigue interaction a simple cumulative damage concept with fractography evidence is used to predict the crack growth rate. It is shown that these models give good agreement with the experimental results.

Keyword: Fracture mechanics, Nickel base supper alloy**,** creep, creep/fatigue interaction, fatigue

INTRODUCTION

Most engineering components which operate at elevated temperatures are subjected to non-steady loading during service. For example, electric power plant may be required to follow the demand for electricity and equipment used for making chemicals may undergo a sequence of operations during the production process. The power plants have to change their operating temperature and pressure to follow the demands of electricity need and to shut down and re-start for their routine maintenance as depicted in Fig. 1. Also, aircraft experience a variety of loading conditions during take-off, flight and landing. There may, in addition, be a superimposed high frequency vibration. Similarly, equipment that is subjected to predominantly steady operating conditions may experience transients during start-up and shut-down. The mechanism of time dependent deformation [1-2] is shown to be analogous to deformation due to plasticity. Therefore elsto-plastic fracture mechanics method can be linked to high temperature fracture mechanics parameters. In this paper techniques are shown for determining the creep fracture mechanics parameter C* using experimental crack growth data.

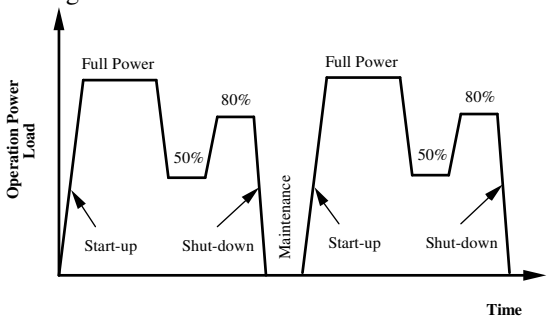

Fig. 1: Example of operation scheme of a power plant

Models for predicting creep crack growth interims of C* and creep uniaxial ductility are discussed. Cumulative damage concept is used for predicting crack growth under static and cyclic loading conditions.

High Temperature Fracture Mechanics: The first analytical study of fracture mechanics was made in the 1920s[3] for cracks in an ideal brittle material. This study was based on the consideration of energy balance in a cracked body. The stress intensity factor K was proposed, as a parameter that describes the stress state around a crack tip, by Irwin [8]. The J contour integral [4] was proposed as a fracture mechanics parameter which has been widely accepted as an effective parameter for the assessment of ductile fracture for large scale yielding cases [2]. In general the more creep ductile the material and the more diffuse the number of cracks or damage region the likelihood that (Non-Linear Fracture Mechanics) NLEFM J at room temperature and C* at high temperature will describe the crack tip region [5,6]. The assumption made is that creep deformation is time dependent. The overriding assumption is that the local crack tip stress singularity will dominate and control the development of the crack under creep. The crack tip singularity, over time, will therefore decrease with increasing ductility in creep producing the same deformation contour as in plasticity

Creep Fracture Mechanics (C* integral): For many materials, creep deformation can be considered to be composed of three regimes, namely primary, secondary and tertiary creep regimes. The secondary creep strain rate can be represented by a power law,

$$\dot{\varepsilon}_s^c = A_s \sigma^{n_s} \quad (1)$$

where A_s, and n_s are material constants. The use of an average creep rate obtained directly from creep rupture

Corresponding Author: F. Djavanroodi, Mechanical Engineering Department, Iran University of Science and Technology(IUST), Narmak, 16844, Tehran, Iran

data has been proposed to account for all three stages of creep [2,5,6].

$$\dot{\varepsilon}_A = \frac{\varepsilon_f}{t_r} = \dot{\varepsilon}_o \left(\frac{\sigma}{\sigma_0} \right)^{n_A} = A_A \sigma^{n_A} \qquad (2)$$

where ε_f is the uniaxial failure strain, t_r is the time to rupture and σ is the applied stress. The variables $\dot{\varepsilon}_o$, σ_o, A_A and n_A in Equation (2) are generally taken as material constants. These equations are used to characterise the steady state (secondary) creep stage where the hardening by dislocation interaction is balanced by recovery processes. The typical value for n is between 3 and 10 for most metals. The definition of the C^* integral is obtained by substituting strain rate and displacement rate for strain and displacement of the J integral [2,5-7].

$$C^* = \int_\Gamma \left[W_s^* dy - T_i (\delta \dot{u}_i / \delta_x) ds \right] \qquad (3)$$

where W^* is strain energy density change rate,

$$W_s^* = \int_o^{\dot{\varepsilon}_{ij}^c} \sigma_{ij} d\dot{\varepsilon}_{ij}^c \qquad (4)$$

where ($\dot{u}_i = du_i / dt$) is displacement rate. The asymptotic stress and strain fields are expressed by equations (5) and (6) [2, 5-7].

$$\sigma_{ij} = \sigma_o \left(\frac{C^*}{I_n \sigma_o \dot{\varepsilon}_o r} \right)^{1/(n+1)} \tilde{\sigma}_{ij}(\theta, n) \qquad (5)$$

$$\dot{\varepsilon}_{ij} = \dot{\varepsilon}_o \left(\frac{C^*}{I_n \sigma_o \dot{\varepsilon}_o r} \right)^{n/(n+1)} \tilde{\varepsilon}_{ij}(\theta, n) \qquad (6)$$

Therefore the stress and strain rate fields of non-linear viscous materials are also HRR type fields with $\tilde{\sigma}_{ij}$ and $\tilde{\varepsilon}_{ij}$ equivalent stress and stain and I_n is the normalizing factor which depends on n and the state of stress.

Experimental Estimate: From the view of an energy balance, the C^* integral is the rate of change of potential energy with crack extension. For any geometry the dimensionalised equation becomes

$$C^* = \frac{n}{n+1} f(a/W) \frac{P\dot{\Delta}}{B_n W} = F \frac{P\dot{\Delta}}{B_n W} \qquad (7)$$

where P is the load, $\dot{\Delta}$ is the displacement rate due to creep, B_n is the net thickness between side grooves, and W is the width of the specimen. The $f(a/W)$ is a non-dimensional geometry function of a crack length a [5-7]. For CT specimens, the $f(a/W)$ is given by analogy with fracture toughness J_{IC} testing in ASTM E813 [7,8].

$$f(a/W) = \frac{2 + 0.552(1 - a/W)}{1 - a/W}$$

Crack growth at elevated temperature: At elevated temperatures where creep is dominant, time-dependent crack growth is observed, creep crack growth rate $\dot{a}$ (= da/dt) is usually given as;

$$\dot{a} = DC^{*\phi} \qquad (9)$$

where D and ϕ are material constants which may depend on temperature and stress state. A suitable parameter to describe crack growth at elevated temperature will depend on material properties, loading condition, and time when crack growth is observed [5, 6].

Modeling of equation (9) can be performed using uniaxial creep properties of material and creep process zone ahead of crack. Nikbin *et al.* [5, 6] used equations (1) to (7) and (9) to develop this model.

$$\dot{a}_s = \frac{(n+1)\dot{\varepsilon}_o}{\varepsilon_f^*} \left[\frac{C^*}{I_n \sigma_o \dot{\varepsilon}_o} \right]^{n/(n+1)} \tilde{\varepsilon}_{ij} \left[r_c^{1/(n+1)} \right] \qquad (10)$$

The non dimensional function $\tilde{\varepsilon}_{ij}$ is normalised so that its maximum equivalent becomes unity. Hence, assuming this maximum value, the constants D and ϕ in equation (9) become;

$$D = \frac{(n+1)\dot{\varepsilon}_o}{\varepsilon_f^*} \left[\frac{1}{I_n \sigma_o \dot{\varepsilon}_o} \right]^{n/n+1} \qquad (11)$$

where $\phi = \frac{n}{n+1}$

In this equation I_n is the normalizing factor which depends on n and the state of stress, r_c is the size of the creep process zone and ε^*_{fo} is equivalent to creep ductility considering constraint effect. For plane stress conditions ε^*_{fo} can be taken as ε_{fo} and for plain strain conditions as $\varepsilon_{fo/50}$.

Fatigue crack growth: Fatigue crack growth is usually observed as transgranular cracking at low temperature. At elevated temperature, transgranular cracks are also observed under relatively high frequency cycles and this fatigue crack growth rate can still be characterised by elastic or elasto-plastic fracture mechanics parameters in most cases [9-11]. The crack growth rate *da/dN* is correlated with ΔK using the power law relation [17] in steady state fatigue as,

$$\frac{da}{dN} = C_f \Delta K^m \qquad R = \frac{\sigma_{\min}}{\sigma_{\max}} \tag{12}$$

where C_f and m are material constants and m is typically around 3. Typically, *da/dN* is sensitive to the mean stress or the load ratio R defined by; $\sigma_{\min}$ and $\sigma_{\max}$ are the minimum stress and the maximum stress, respectively[9]. As temperature is increased, time dependent processes become more significant. Creep and environmentally assisted crack growth can take place more readily since they are aided by diffusion and rates of diffusion increase with rise in temperature. Generally the influence of frequency on crack propagation rate is more pronounced with increase in temperature and R [9-11]. Figure 2 shows a schematic description of cracking rate versus ΔK for cyclic cracking at elevated temperatures showing the effects of frequency, R-ratio and temperature.

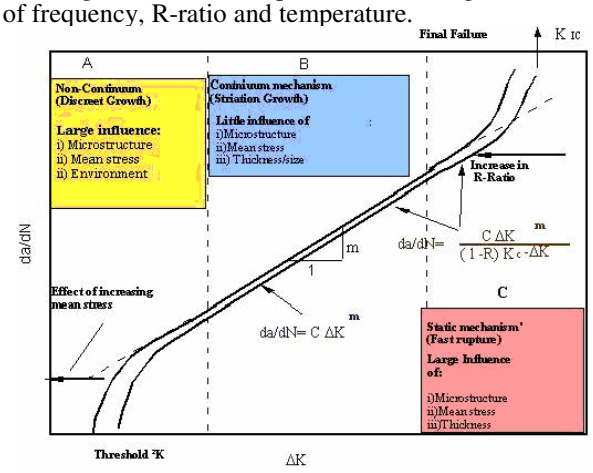

Fig. 2: Cyclic crack growth at elevated temperatures

Creep-fatigue crack growth: As it is shown in Fig. 1 interaction between creep and fatigue is expected under cyclic loading. Some of the causes of creep-fatigue interaction might be the enhancement of fatigue crack growth due to embrittlement of grain boundaries or weakening of the matrix in grains and enhancement of creep crack growth due to acceleration of precipitation or cavitation by cyclic loading [12-14]. Nevertheless, it has been proposed that a simple linear summation rule for creep-fatigue crack growth can be applied to predict the crack growth.

$$\frac{da}{dN} = \left(\frac{da}{dN}\right)_{creep} + \left(\frac{da}{dN}\right)_{fatigue} = \frac{1}{3600f}\left(\frac{da}{dt}\right)_{creep} + \left(\frac{da}{dN}\right)_{fatigue} \tag{13}$$

$$\frac{da}{dt} = \left(\frac{da}{dt}\right)_{creep} + \left(\frac{da}{dt}\right)_{fatigue} = \left(\frac{da}{dt}\right)_{creep} + 3600f\left(\frac{da}{dN}\right)_{fatigue} \tag{14}$$

where *da/dN* is crack growth per cycle (mm/cycle), *da/dt* is crack growth rate in mm/hour, and f is frequency in Hz.

Table 1: Nickel base supper alloy

Cr	Co	Mo	Ti	Al	Zr	C	Ni
14.8	16.9	5.04	3.52	3.98	0.44	0.022	Balance

Heat treatment: 4 hours at 1100°C – Air cooled-Tempered, 24 hours at 650°C – Air cooled – Tempered, 8 hours at 760°C – Air cooled

MATERIALS AND METHOD

The chemical compositions and heat treatments for the material used for experimental work are presented in table 1. The supper alloy was received in form of hot isostatically pressed billets which had been heat treated to produce a microstructure containing approximately 40% vol of gama phase dispersed in a gama-nickel solid solution matrix and grain size of 60 um. It was tested at temperature of 700°C. At this temperature it had a uniaxial creep ductility of about 15% and material hardness was around 470 VHN. Detail of experimental procedure has been presented previously[15]. Only outline will be included here. Specimens used for investigation were Single Edge Notched Tension (SENT) with W = 20 mm and thickness B = 5mm and Compact Tension with W = 50mm and B = 25mm the testing was performed at 700°C. Crack growth

experiment has been conducted over a range of frequencies between 10 and 10 Hz. During each test displacement was measured continuously with electrical transducer and crack extension by a combination of optical and electrical potential difference method to an estimated accuracy of +0.1 mm. The wave shape employed was sinusoidal for frequencies of 0.1 Hz and greater, and square-wave for frequencies lower than this. Experimental results and discussion: Effects of the influence of frequency on crack growth/cycle in a nickel base alloy at 700°C at R = 0.7 is shown in Fig. 4. In the steady state cracking region crack growth can be described by the Paris law (equation (12)) with m ≈ 2.5. This value is within the range expected for room temperature behaviour. Correlation of results obtained at 20

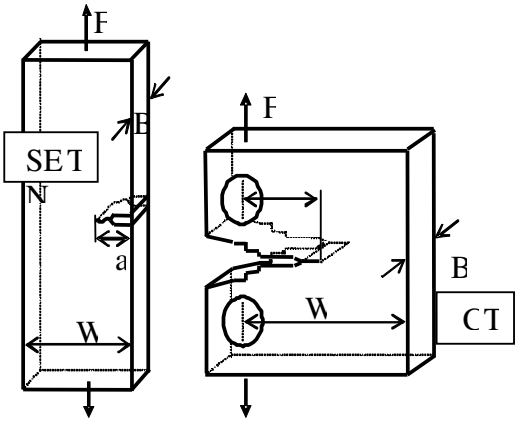

Fig. 3: Single Edge Notch Tension (SENT) and Compact Tension (CT) specimens

Mpa√m for specimen thickness (B=25mm) is depicted in Fig. 4. Furthermore in Fig. 5 the two lines show the relative behaviour of the creep and the fatigue components of da/dN. The slope of -1 indicates time dependent creep cracking and the horizontal line indicates fatigue control of da/dN. Therefore by adding the two components it is clear that at high frequency creep is seen to have third order effect on cracking rate and conversely at low frequencies fatigue has a third order effect. From metallurgical and fractographic investigations performed on the alloy tested in the creep and creep fatigue range similar qualitative conclusions can be reached with respect to the mode of the creep fatigue interaction.

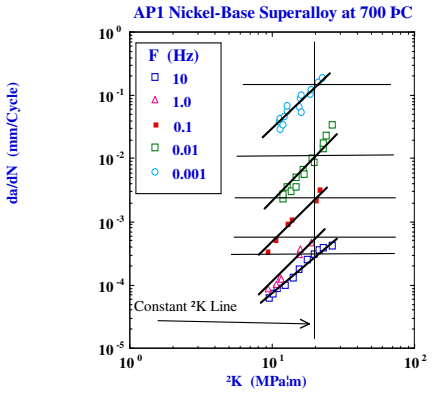

Fig. 4: Frequency dependence of fatigue cracking at high temperatures for nickel-base superally tested at 700 °C and R=0.7

Fig. 6 show the fractographs for the nickel-base superalloy tested at 700 °C. There is a transition from intergranular cracking at f=0.001 Hz to transgranular cracking at 10 Hz.

The intermediate frequencies show a mixture of intergranular and transgranular cracking modes. These suggest that the two mechanism work in parallel and that cumulative damage concepts proposed above can well describe the total cracking behaviour. In this region crack growth can be described by equation (13).

The effects of R-ratio on creep/fatigue interaction is shown in Figs. 7 and 8. Generally as shown in Fig. 7 an increase in the R-ratio reduces the ΔK needed for crack growth per cycle and increase in frequency reduced the *da/dN*.

Fig. 8 a,b compare the *da/dN* in terms of frequency in terms of constant ΔK and constant *Kmax*. Fig. 8a shows a dependence of *da/dN* versus

$$da/daN = (da/dN) + (da/dt)/f$$

Total = Fatigue + Creep

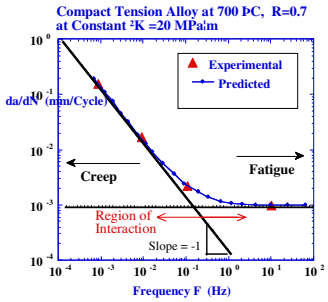

Fig. 5: Fatigue crack growth sensitivity to frequency in nickel-base superalloy tested at 700 °C.

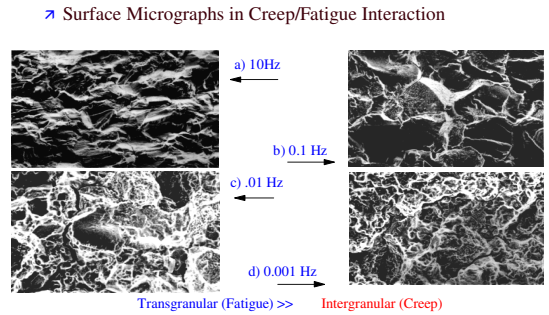

Fig. 6: Effects of frequency on mode of failure for Nickel-base superalloy tested at 700 °C.

frequency on R-ratio. It is clear that at low frequencies cracking is independent of R-ratio when plotted in terms of *Kmax* as shown in Fig. 8b. This suggests that creep failure dominates at maximum load for low frequencies.

In both Figs. 5 and 8 it is clear that the interaction region of creep fatigue is contained within a small frequency band of 1 decade in the region of 0.1 to 1 Hz. From experimental and data analysis performed [13 - 15] it has been shown that static crack growth data correlates well with low frequency (= 0.001 Hz) data. Therefore equations (13-14) can be used to incorporate static data with cyclic data. This method is useful for cases where no cyclic data exists and only static and high frequency data is available.

The effects of constraint due to geometry and specimen size can be described using the cumulative method and over a range of frequencies or using C* at low frequencies where creep dominates. Fig. 9 shows the effects of geometry and specimen size on crack

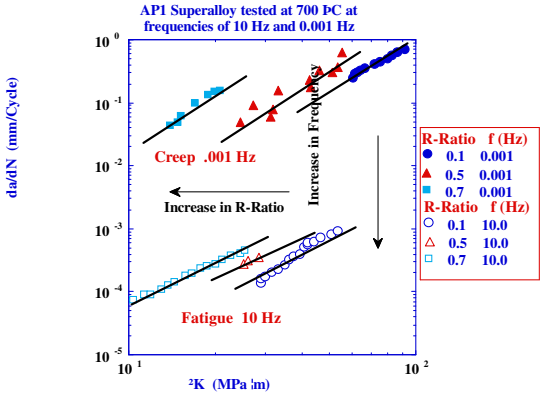

Fig 7: Dependence of crack growth on frequency and R-Ratio for nickel-base superalloy tested at 700 °C.

growth at constant ΔK over a range of frequencies for the alloy at 700 °C.

At high frequencies there are no size and geometry effects however at low frequencies the Single Edge Notch Tension (SENT) specimens, shown in Fig. 9 exhibit lower *da/dN* compared to the thin CT specimens and this in turn shows a lower *da/dN* compared to the 25mm thick CT. Therefore constraint effects are exaggerated under creep conditions and increase in constraint tends to increase cracking rates.

Figure 10 shows, Predictions of crack growth rate versus C* for nickel-base superally tested at 700 °C using the steady state model plain stress and strain condition, as it can bee seen that model bounds the steady state crack growth rates. Also the effects ofgeometry and specimen size on creep crack growth for the alloy is shown in Fig. 10. It is clear that cracking rate is state of stress controlled in the creep range.

CONCLUSION

It has been shown that high-temperature crack growth occurs by either cyclic-controlled or time-dependent processes. Over the limited range where both are significant, a simple cumulative damage law can be employed to predict behaviour. Interpretations have been developed in terms of linear elastic and non linear fracture mechanics concepts. Linear elastic fracture mechanics descriptions are expected to be adequate when fatigue and environmental processes dominate. When creep mechanisms control stress redistribution

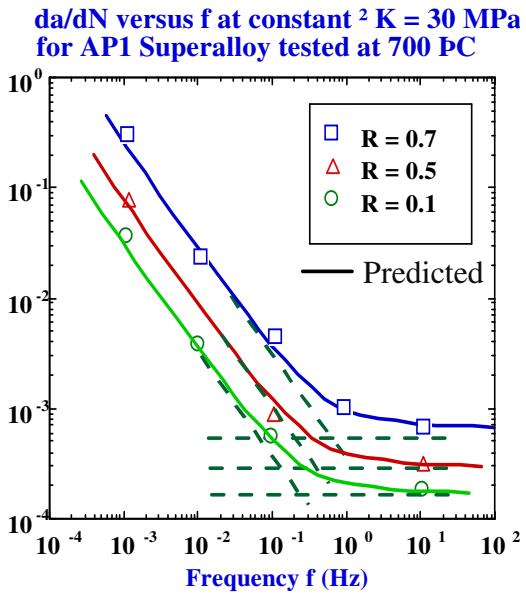

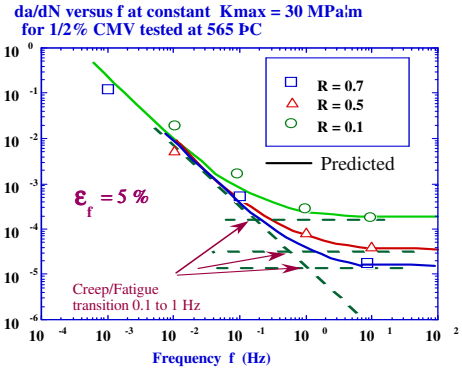

Fig. 8: Fatigue crack growth sensitivity to frequency and R-ratio in nickel-base superalloy tested at 700 °C at a) constant ΔK=30MPa√m and b) constant Kmax= 30MPa√m

takes place in the vicinity of the crack tip and use of the creep fracture mechanics parameter C* should be employed for characterising the creep component of cracking.

In the region where the Paris law is relevant, substitution of the C* relation to crack growth into equation (13) allows cyclic crack growth under creep-fatigue loading conditions to be established from

$$da/dN = C\Delta K^{m} + DC^{*\phi}/f \quad (15)$$

where da/dN is in mm/cycle with frequency in Hz. To allow for crack closure effects, ΔK in these equations can be replaced by ΔK_{eff}. Similarly ΔJ can be used instead of ΔK when plastic deformation is significant. In order to make predictions of creep-fatigue crack growth in components it is necessary to be able to calculate ΔK and C^* as crack advance occurs

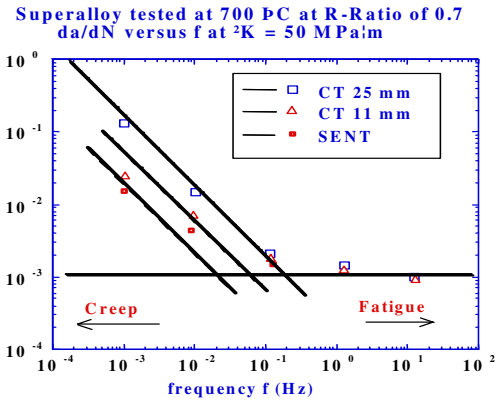

Fig 9: Geometry and size effects in the creep/fatigue crack growth of nickel base superalloy tested at 700 °C.

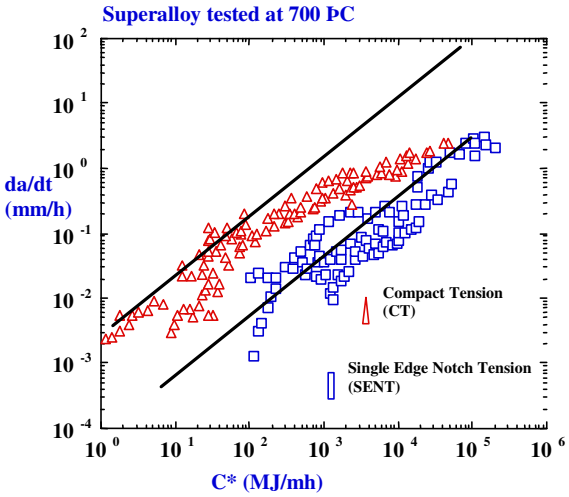

Fig. 10: Effect of geometry in creep crack growth of Nickel-base superalloy tested at 700 °C

REFERENCES

1. Riedel, H., 1987. Fracture at high temperatures: Springer-Verlag, Berlin.
2. Webster, G. A., And Ainsworth, R. A, 1994. high temperature component life assessment: Chapman & Hall.
3. Irwin, B, 1948. Fracture dynamics, in Fracturing of metals: ASM, p. 147-166.
4. Rice, J. R, 1968. A Path Independent Integral and the Approximate Analysis of Strain Concentration by Notches and Cracks: Journal of Applied Mechanics, E35(ASME): p. 379-386.
5. Nikbin, K. M., Smith, D. J., and Webster, G. A, 1984. Prediction of Creep Crack Growth From Uniaxial Creep Data: Proc. of Royal Society, London, A396: p. 183-197.
6. Nikbin, K. M., Smith, D. J., and Webster, G. A., 1986. An Engineering Approach to the Prediction of Creep Crack Growth: J. of Eng. Mat. and Tech. ASME, 108: p. 186-191.
7. ASTM E 1457-00, 2001. Standard Test Method for Measurement of Creep Crack Growth Rates in Metals: Annual Book of ASTM Standards, Vol. 3, no. 1, pp. 936-950.
8. ASTM, 1987. Standard Test for JIC, a Measure of Fracture Toughness: ASTM E813.
9. Paris, P. C, 1977. Fracture Mechanics in the Elastic Plastic Regime. ASTM STP, 631 American society for Testing and Materials: p. 3-27.

10. Forman, R. G., Kearney, V. E., and Engle, R. M., 1967. Numerical analysis of Crack Propagation in a Cyclic-loaded Structures: ASME Transaction, Journal of Basic Engineering, 89(D): p. 459.
11. Paris, P. C., Gomez, M. P., and Anderson, W. E., A 1961. Rational Analytic Theory of Fatigue: Trend in Engineering, 13: p. 9-14.
12. Nikbin, K.M. and Webster, G.A., 1984. Creep-fatigue crack growth in a nickel base superalloy, in Creep and fracture of engineering materials and structures, (Eds B. Wilshire and D.R.J. Owen). Pineridge Press, Swansea, 1091-1103.
13. Winstone, M.R., Nikbin, K.M. and Webster, G.A., 1985. Modes of failure under creep/fatigue loading of a nickel-base superalloy: J. Matls Sci,, 20, 2471-2476.
14. Dimopulos, V., Nikbin, K.M. and Webster, G.A. 1988. Influence of cyclic to mean load ratio on creep/fatigue crack growth: Met. Trans. A, , 19A, 873-880.
15. Smith, D. J., and Webster, G. A, 1984. Mechanical Behaviour of Materials IV, Ed. J. Carlson and N. G. Ohlson: Pergamon Press, Oxford, 315 – 321,